

## Optical tweezers computational toolbox

To cite this article: Timo A Nieminen *et al* 2007 *J. Opt. A: Pure Appl. Opt.* **9** S196

View the [article online](#) for updates and enhancements.

### You may also like

- [iEEGview: an open-source multifunction GUI-based Matlab toolbox for localization and visualization of human intracranial electrodes](#)  
Guangye Li, Shize Jiang, Chen Chen et al.
- [An open source benchmarked toolbox for cardiovascular waveform and interval analysis](#)  
Adriana N Vest, Giulia Da Poian, Qiao Li et al.
- [Gumpy: a Python toolbox suitable for hybrid brain-computer interfaces](#)  
Zied Tayeb, Nicolai Waniek, Juri Fedjaev et al.

# Optical tweezers computational toolbox

**Timo A Nieminen, Vincent L Y Loke, Alexander B Stilgoe,  
Gregor Knöner, Agata M Brańczyk, Norman R Heckenberg and  
Halina Rubinsztein-Dunlop**

Centre for Biophotonics and Laser Science, School of Physical Sciences, The University of  
Queensland, Brisbane QLD 4072, Australia

Received 5 March 2007, accepted for publication 13 April 2007

Published 24 July 2007

Online at [stacks.iop.org/JOptA/9/S196](http://stacks.iop.org/JOptA/9/S196)

## Abstract

We describe a toolbox, implemented in Matlab, for the computational modelling of optical tweezers. The toolbox is designed for the calculation of optical forces and torques, and can be used for both spherical and nonspherical particles, in both Gaussian and other beams. The toolbox might also be useful for light scattering using either Lorenz–Mie theory or the  $T$ -matrix method.

**Keywords:** optical tweezers, laser trapping, light scattering, Mie theory,  $T$ -matrix method

(Some figures in this article are in colour only in the electronic version)

## 1. Introduction

Computational modelling provides an important bridge between theory and experiment—apart from the simplest cases, computational methods must be used to obtain quantitative results from theory for comparison with experimental results. This is very much the case for optical trapping, where the size range of typical particles trapped and manipulated in optical tweezers occupies the gap between the geometric optics and Rayleigh scattering regimes, necessitating the application of electromagnetic theory. Although, in principle, the simplest cases—the trapping and manipulation of homogeneous and isotropic microspheres—have an analytical solution—generalized Lorenz–Mie theory, significant computational effort is still required to obtain quantitative results. Unfortunately, the mathematical complexity of Lorenz–Mie theory presents a significant barrier to entry for the novice, and is likely to be a major contributor to the lagging of rigorous computational modelling of optical tweezers compared to experiment.

If we further consider the calculation of optical forces and torques on non-spherical particles—for example, if we wish to consider optical torques on and rotational alignment of non-spherical microparticles, the mathematical difficulty is considerably greater. Interestingly, one of the most efficient methods for calculating optical forces and torques on non-spherical particles in optical traps is closely allied to Lorenz–Mie theory—the  $T$ -matrix method (Waterman 1971,

Mishchenko 1991, Nieminen *et al* 2003a). However, while the Mie scattering coefficients have a relatively simple analytical form, albeit involving special functions, the  $T$ -matrix requires considerable numerical effort for its calculation. It is not surprising that the comprehensive bibliographic database on computational light scattering using the  $T$ -matrix method by Mishchenko *et al* (2004) lists only four papers applying the method to optical tweezers (Bayouth *et al* 2003, Bishop *et al* 2003, Nieminen *et al* 2001a, 2001b). Since the compilation of this bibliography, other papers have appeared in which this is done (Nieminen *et al* 2004, Simpson and Hanna 2007, Singer *et al* 2006), but they are few in number.

Since the potential benefits of precise and accurate computational modelling of optical trapping is clear, both for spherical and non-spherical particles, we believe that the release of a freely available computational toolbox will be valuable to the optical trapping community.

We describe such a toolbox, implemented in Matlab. We outline the theory underlying the computational methods, the mathematics and the algorithms, the toolbox itself, and typical usage, and present some example results. The toolbox can be obtained at <http://www.physics.uq.edu.au/people/nieminen/software.html> at the time of publication. Since such software projects tend to evolve over time, and we certainly intend that this one will do so, potential users are advised to check the accompanying documentation. Along these lines, we describe our plans for future development. Of course, we welcome input, feedback, and contributions from the optical trapping community.

## 2. Fundamentals

### 2.1. Optical tweezers as a scattering problem and the $T$ -matrix method

The optical forces and torques that allow trapping and manipulation of microparticles in beams of light result from the transfer of momentum and angular momentum from the electromagnetic field to the particle—the particle alters the momentum or angular momentum flux of the beam through scattering. Thus, the problem of calculating optical forces and torques is essentially a problem of computational light scattering. In some ways, it is a simple problem: the incident field is monochromatic, there is usually only a single trapped particle, which is finite in extent, and speeds are so much smaller than the speed of light that we can for most purposes neglect Doppler shifts and assume we have a steady-state monochromatic single-scattering problem.

Although typical particles inconveniently are of sizes lying within the gap between the regimes of applicability of small-particle approximations (Rayleigh scattering) and large-particle approximations (geometric optics), the particles of choice are often homogeneous isotropic spheres, for which an analytical solution to the scattering problem is available—the Lorenz–Mie solution (Lorenz 1890, Mie 1908). While the application of Lorenz–Mie theory requires significant computational effort, the methods are well known.

The greatest difficulty encountered results from the incident beam being a tightly focused beam. The original Lorenz–Mie theory was developed for scattering of plane waves, and its extension to non-plane illumination is usually called generalized Lorenz–Mie theory (GLMT) (Gouesbet and Grehan 1982), which has seen significant use for modelling the optical trapping of homogeneous isotropic spheres (Ren *et al* 1996, Wohland *et al* 1996, Maia Neto and Nussenzweig 2000, Mazolli *et al* 2003, Lock 2004a, 2004b, Knöner *et al* 2006, Neves *et al* 2006). The same name is sometimes used for the extension of Lorenz–Mie theory to non-spherical, but still separable, geometries such as spheroids (Han and Wu 2001, Han *et al* 2003).

The source of the difficulty lies in the usual paraxial representations of laser beams being solutions of the scalar paraxial wave equation rather than solutions of the vector Helmholtz equation. Our method of choice is to use a least-squares fit to produce a Helmholtz beam with a far field matching that expected from the incident beam being focused by the objective (Nieminen *et al* 2003b).

At this point, we can write the incident field in terms of a discrete basis set of functions  $\psi_n^{(\text{inc})}$ , where  $n$  is the mode index labelling the functions, each of which is a solution of the Helmholtz equation,

$$U_{\text{inc}} = \sum_n a_n \psi_n^{(\text{inc})}, \quad (1)$$

where  $a_n$  are the expansion coefficients for the incident wave. In practice, the sum must be truncated at some finite  $n_{\text{max}}$ , which places restrictions on the convergence behaviour of useful basis sets. A similar expansion is possible for the scattered wave, and we can write

$$U_{\text{scat}} = \sum_k p_k \psi_k^{(\text{scat})}, \quad (2)$$

where  $p_k$  are the expansion coefficients for the scattered wave.

As long as the response of the scatterer—the trapped particle in this case—is linear, the relation between the incident and scattered fields must be linear, and can be written as a simple matrix equation

$$p_k = \sum_n T_{kn} a_n \quad (3)$$

or, in more concise notation,

$$\mathbf{P} = \mathbf{T}\mathbf{A} \quad (4)$$

where  $T_{kn}$  are the elements of the  $T$ -matrix. This is the foundation of both GLMT and the  $T$ -matrix method. In GLMT, the  $T$ -matrix  $\mathbf{T}$  is diagonal, whereas for non-spherical particles, it is not.

When the scatterer is finite and compact, the most useful set of basis functions is vector spherical wavefunctions (VSWFs) (Waterman 1971, Mishchenko 1991, Nieminen *et al* 2003a, 2003b). Since the VSWFs are a discrete basis, this method lends itself well to representation of the fields on a digital computer, especially since their convergence is well behaved and known (Brock 2001).

The  $T$ -matrix depends only on the properties of the particle—its composition, size, shape, and orientation—and the wavelength, and is otherwise independent of the incident field. This means that for any particular particle the  $T$ -matrix only needs to be calculated once, and can then be used for repeated calculations of optical force and torque. This is the key point that makes this a highly attractive method for modelling optical trapping and micromanipulation, since we are typically interested in the optical force and torque as a function of position within the trap, even if we are merely trying to find the equilibrium position and orientation within the trap. Thus, calculations must be performed for varying incident illumination, which can be done very easily with the  $T$ -matrix method. This provides a significant advantage over many other methods of calculating scattering, where the entire calculation needs to be repeated. This is perhaps the reason that while optical forces and torques have been successfully modelled using methods such as the finite-difference time-domain method (FDTD), the finite-element method (FEM), or other methods (White 2000a, 2000b, Hoekstra *et al* 2001, Collett *et al* 2003, Gauthier 2005, Chaumet *et al* 2005, Sun *et al* 2006, Wong and Ratner 2006), the practical application of such work has been limited.

Since, as noted above, the optical forces and torques result from differences between the incoming and outgoing fluxes of electromagnetic momentum and angular momentum, calculation of these fluxes is required. This can be done by integration of the Maxwell stress tensor, and its moment for the torque, over a surface surrounding the particle. Fortunately, in the  $T$ -matrix method, the bulk of this integral can be performed analytically, exploiting the orthogonality properties of the VSWFs. In this way, the calculation can be reduced to sums of products of the expansion coefficients of the fields.

## 2.2. Controversies in electromagnetic theory

At this point, two controversies in macroscopic classical electromagnetic theory intrude. The first of these is the Abraham–Minkowski controversy, concerning the momentum of an electromagnetic wave in a material medium (Minkowski 1908, Abraham 1909, 1910, Jackson 1999, Pfeifer *et al* 2006, Leonhardt 2006). Abraham’s approach can be summarized as calling  $P/nc$  the electromagnetic momentum flux, where  $P$  is the power,  $n$  the refractive index, and  $c$  the speed of light in free space. The quantum equivalent is the momentum of a photon in a material medium being  $\hbar k/n^2 = \hbar k_0/n$ . Minkowski, on the other hand, gives  $nP/c$  as the electromagnetic momentum flux, or  $\hbar k = n\hbar k_0$  per photon.

While the difference between these two might seem disconcerting when one is intending to calculate the optical force on a particle in a dielectric medium, it is necessary to realize that we are not seeking the *electromagnetic* force but the *total* force due to the incident beam. At least as far as optical tweezers are concerned, where we have time-harmonic steady-state illumination in a medium that can be simply characterized by a refractive index, and are satisfied with the time-averaged force, the total force is the same regardless of our choice of the Abraham or Minkowski expression for the momentum (Jones 1978).

In the Minkowski picture, in our circumstances, other than the refractive index of the medium not being equal to one, the stationary medium is treated identically to free space. Thus, the total momentum is equal to the Minkowski momentum  $nP/c$ .

In the Abraham picture, on the other hand, we find a more physical view of the medium, and the electromagnetic momentum of the wave and the momentum carried by the wave of induced dielectric polarization are considered separately. The sum of these momenta is equal to, again, the Minkowski momentum  $nP/c$ .

Thus, for practical purposes, we take  $nP/c$  to be the total momentum flux.

The second controversy is the angular momentum density of circularly polarized electromagnetic waves (Humblet 1943, Stewart 2005, Pfeifer *et al* 2006). On the one hand, we can begin with the assumption that the angular momentum density is the moment of the momentum density,  $\mathbf{r} \times (\mathbf{E} \times \mathbf{H})/c$ , which results in a circularly polarized plane wave carrying zero angular momentum in the direction of propagation. On the other hand, we can begin with the Lagrangian for an electromagnetic radiation field, and obtain the canonical stress tensor and an angular momentum tensor that can be divided into spin and orbital components (Jauch and Rohrlich 1976). For a circularly polarized plane wave, the component of the angular momentum flux in the direction of propagation would be  $I/\omega$ , where  $I$  is the irradiance and  $\omega$  the angular frequency, in disagreement with the first result.

However, it is not the angular momentum density as such that we are interested in, but the total angular momentum flux through a spherical surface surrounding the particle, which is equal to the torque exerted on the trapped particle. For the electromagnetic fields used in optical tweezers, this integrated flux is the same for both choices of angular momentum density (Humblet 1943, Crichton and Marston 2000, Zambrini and Barnett 2005). Since the formula given in section 5 for the

torque is for the total angular momentum flux, it is unaffected by this controversy.

Crichton and Marston (2000) also show that for monochromatic radiation the division into spin and orbital angular momenta is gauge invariant, and observable, with it being possible to obtain the spin from measurement of the Stokes parameters. Since the torque due to spin is of practical interest (Nieminen *et al* 2001a, Bishop *et al* 2003, 2004), it is worthwhile to calculate this as well as the total torque.

Whether or not the angular momentum flux is altered by the presence of a dielectric medium has also been considered (Padgett *et al* 2003, Mansuripur 2005), essentially an angular momentum version of the Abraham–Minkowski controversy. As far as optical tweezers are concerned, it is immaterial whether or not the angular momentum is carried electromagnetically or by the medium, as long as we know the total rate of transfer of angular momentum to the particle in the trap. Where the total momentum flux is given by the Minkowski momentum, the total angular momentum flux is unchanged by entry into a dielectric medium (Brevik 1979, Padgett *et al* 2003). Thus, we can take the total angular momentum flux of a circularly polarized finite beam to be  $P/\omega$ , whether it is in free space or a dielectric medium.

## 2.3. Further reading

The mathematics of optical tweezers is largely that of light scattering. The literature on scattering is extensive, often highly specialized, and frequently difficult to digest. Fortunately for the newcomer, Bohren (1995) gives an engaging and accessible introduction. The classic treatise by van de Hulst (1957) is another good starting point, especially for its lucid coverage of Lorenz–Mie theory.

The  $T$ -matrix method is often used synonymously to mean the extended boundary condition method (EBCM), introduced by Waterman (1971) as a method to calculate the  $T$ -matrix. However, the EBCM is just that—a method which one can use to calculate the  $T$ -matrix—and the  $T$ -matrix method is more general, as pointed out by Kahnert (2003) and Nieminen *et al* (2003a). The  $T$ -matrix method is described by Mishchenko *et al* (2002) and Tsang (2001), and the interested reader can consult the bibliography by Mishchenko *et al* (2004) for other works.

We recommend the review by Kahnert (2003) for readers interested in a more general coverage of numerical methods in light scattering, including FDTD and FEM. The shorter review by Wriedt (1998) may also be of interest.

The reader may well come to the conclusion that the  $T$ -matrix method is more mathematically esoteric than most other methods. This is, unfortunately, the price we pay for its strengths, which include, in addition to the previously mentioned efficiency with regard to repeated calculations for the same particle and the ease of calculating the force and torque from the fields, it being naturally suited to scattering in open domains.

Apart from the works noted earlier, in which Lorenz–Mie theory, the  $T$ -matrix method, or some other rigorous electromagnetic method is used to calculate optical forces in optical tweezers, we can also mention related works. Firstly, the  $T$ -matrix method has been used for the calculation of forces

in optical binding (Simpson and Hanna 2006, Grzegorzczuk *et al* 2006).

Secondly, approximate methods such as geometric optics or Rayleigh scattering can also prove useful, for large and small particles respectively. The classic paper by Ashkin (1992) is an excellent introduction to the modelling of optical tweezers using geometric optics, and Harada and Asakura (1996) discuss forces in the Rayleigh regime and the limits of applicability of the Rayleigh approximation in optical tweezers.

Although the practical impact of the Abraham–Minkowski and angular momentum controversies on optical tweezers is negligible, the converse does not appear to be true—the controversies continue to be debated, more actively than ever before, and this appears to be driven at least in part by the widespread application of electromagnetic forces and torques in optical tweezers.

In our opinion, the Abraham–Minkowski controversy is essentially one of semantics—what portion of the total momentum is to be labelled ‘electromagnetic’, and what portion is to be labelled ‘material’; Penfield and Haus (1967), de Groot and Suttrop (1972), Gordon (1973), and others have shown that the division of the total energy–momentum tensor into electromagnetic and material parts is effectively arbitrary (Pfeifer *et al* 2006). That the transport of energy necessitates the transfer of momentum, with a momentum flux of  $P/v$ , where  $v$  is the speed of energy transport, was shown as long ago as 1873 by Umov, with the result that the Minkowski momentum gives the total momentum flux. Unfortunately, Umov’s work does not seem to be readily available in English (Umov 1950).

In the context of optical tweezers, Gordon’s (1973) work is usefully enlightening. We can consider a finite beam passing through a medium composed of molecules. At the edges of the beam, where  $\nabla|\mathbf{E}|^2$  is non-zero, an optical gradient force will act on the molecules. However, in a steady-state case, the net force must be zero. Since the only forces acting on the molecules at the edge of the beam are the electromagnetic force and forces due to the surrounding molecules—pressure, there must be an increase in pressure within the beam. If a particle is trapped by the beam, the force exerted on the particle will be the sum of the electromagnetic force and this pressure force, the total being equal to the change in the Minkowski momentum.

Nonetheless, the controversy continues to be actively debated (Mansuripur 2004, Barnett and Loudon 2006, Leonhardt 2006, Mansuripur 2007, Loudon and Barnett 2006). Clearly, the last word is yet to be said on this issue.

The second controversy, concerning angular momentum, appears to arise from two sources. Firstly, it is natural to assume that the angular momentum density is  $\mathbf{r} \times (\mathbf{E} \times \mathbf{H})/c$ . Secondly, the conservation law for angular momentum obtained via Lagrangian field theory is for the total angular momentum, and identification of the integrand in the integral as the angular momentum density is uncertain.

As far as the total angular momentum flux is concerned, both pictures give exactly the same result for a bounded beam (Humblet 1943, Soper 1976). Jackson (1999) gives a problem (7.28) allowing the student to explicitly demonstrate this. The division of the angular momentum density of an

electromagnetic field into spin and orbital parts is, in general, not gauge invariant, and it is common to transform the integral of the angular momentum density into a gauge-invariant form, yielding the integral of  $\mathbf{r} \times (\mathbf{E} \times \mathbf{H})/c$ . Jauch and Rohrlich (1976) carefully point out that this transformation requires the dropping of surface terms at infinity. The reverse of this procedure, obtaining the spin and orbital term starting from  $\mathbf{r} \times (\mathbf{E} \times \mathbf{H})/c$ , involving the same surface terms, had already been shown by Humblet (1943). These surface terms disappear for finite beams and only in the case of an unbounded wave—such as an infinite plane wave—does a possible discrepancy exist.

The gauge invariance of the separation of the angular momentum into spin and orbital angular momentum has also attracted attention. However, this does not affect the torque exerted on a particle, and, in any case, the separation appears to be gauge invariant for a monochromatic wave (Crichton and Marston 2000, Barnett 2002).

### 3. Incident field

The natural choice of coordinate system for optical tweezers is spherical coordinates centred on the trapped particle. Thus, the incoming and outgoing fields can be expanded in terms of incoming and outgoing vector spherical wavefunctions (VSWFs):

$$\mathbf{E}_{\text{in}} = \sum_{n=1}^{\infty} \sum_{m=-n}^n a_{nm} \mathbf{M}_{nm}^{(2)}(k\mathbf{r}) + b_{nm} \mathbf{N}_{nm}^{(2)}(k\mathbf{r}), \quad (5)$$

$$\mathbf{E}_{\text{out}} = \sum_{n=1}^{\infty} \sum_{m=-n}^n p_{nm} \mathbf{M}_{nm}^{(1)}(k\mathbf{r}) + q_{nm} \mathbf{N}_{nm}^{(1)}(k\mathbf{r}) \quad (6)$$

where the VSWFs are

$$\begin{aligned} \mathbf{M}_{nm}^{(1,2)}(k\mathbf{r}) &= N_n h_n^{(1,2)}(kr) \mathbf{C}_{nm}(\theta, \phi) \\ \mathbf{N}_{nm}^{(1,2)}(k\mathbf{r}) &= \frac{h_n^{(1,2)}(kr)}{kr N_n} \mathbf{P}_{nm}(\theta, \phi) \\ &+ N_n \left( h_{n-1}^{(1,2)}(kr) - \frac{nh_n^{(1,2)}(kr)}{kr} \right) \mathbf{B}_{nm}(\theta, \phi) \end{aligned} \quad (7)$$

where  $h_n^{(1,2)}(kr)$  are spherical Hankel functions of the first and second kinds,  $N_n = [n(n+1)]^{-1/2}$  are normalization constants,  $\mathbf{B}_{nm}(\theta, \phi) = \mathbf{r} \nabla Y_n^m(\theta, \phi)$ ,  $\mathbf{C}_{nm}(\theta, \phi) = \nabla \times (\mathbf{r} Y_n^m(\theta, \phi))$ , and  $\mathbf{P}_{nm}(\theta, \phi) = \hat{\mathbf{r}} Y_n^m(\theta, \phi)$  are the vector spherical harmonics (Waterman 1971, Mishchenko 1991, Nieminen *et al* 2003a, 2003b), and  $Y_n^m(\theta, \phi)$  are normalized scalar spherical harmonics. The usual polar spherical coordinates are used, where  $\theta$  is the co-latitude, measured from the  $+z$  axis, and  $\phi$  is the azimuth, measured from the  $+x$  axis towards the  $+y$  axis.

$\mathbf{M}_{nm}^{(1)}$  and  $\mathbf{N}_{nm}^{(1)}$  are outward-propagating TE and TM multipole fields, while  $\mathbf{M}_{nm}^{(2)}$  and  $\mathbf{N}_{nm}^{(2)}$  are the corresponding inward-propagating multipole fields. Since these wavefunctions are purely incoming and purely outgoing, each has a singularity at the origin. Since fields that are free of singularities are of interest, it is useful to define the singularity-free regular vector spherical wavefunctions:

$$\mathbf{RgM}_{nm}(kr) = \frac{1}{2}[\mathbf{M}_{nm}^{(1)}(kr) + \mathbf{M}_{nm}^{(2)}(kr)], \quad (8)$$



$$\mathbf{RgN}_{nm}(kr) = \frac{1}{2}[\mathbf{N}_{nm}^{(1)}(kr) + \mathbf{N}_{nm}^{(2)}(kr)]. \quad (9)$$

Although it is usual to expand the incident field in terms of the regular VSWFs, and the scattered field in terms of outgoing VSWFs, this results in both the incident and scattered waves carrying momentum and angular momentum away from the system. Since we are primarily interested in the transport of momentum and angular momentum by the fields (and energy, too, if the particle is absorbing), we separate the total field into purely incoming and outgoing portions in order to calculate these. The user of the code can choose whether the incident–scattered or incoming–outgoing representation is used otherwise.

We use an over-determined point-matching scheme to find the expansion coefficients  $a_{nm}$  and  $b_{nm}$  describing the incident beam (Nieminen *et al* 2003b), providing stable and robust numerical performance and convergence.

Finally, one needs to be able to calculate the force and torque for the same particle in the same trapping beam, but at different positions or orientations. The transformations of the VSWFs under rotation of the coordinate system or translation of the origin of the coordinate system are known (Brock 2001, Videen 2000, Gumerov and Duraiswami 2003, Choi *et al* 1999). It is sufficient to find the VSWF expansion of the incident beam for a single origin and orientation, and then use translations and rotations to find the new VSWF expansions about other points (Nieminen *et al* 2003b, Doicu and Wriedt 1997, Moine and Stout 2005). Since the transformation matrices for rotation and translations along the  $z$ -axis are sparse, while the transformation matrices for arbitrary translations are full, the most efficient way to carry out an arbitrary translation is by a combination of rotation and axial translation. The transformation matrices for both rotations and axial translations can be efficiently computed using recursive methods (Videen 2000, Gumerov and Duraiswami 2003, Choi *et al* 1999).

### 3.1. Implementation

Firstly, it is necessary to provide routines to calculate the special functions involved. These include the following.

- (i) `sbesselj.m`, `sbesselh.m`, `sbesselh1.m`, and `sbesselh2.m` for the calculation of spherical Bessel and Hankel functions. These make use of the Matlab functions for cylindrical Bessel functions.
- (ii) `sparm.m` for scalar spherical harmonics and their angular partial derivatives.
- (iii) `vsh.m` for vector spherical harmonics.
- (iv) `vswf.m` for vector spherical wavefunctions.

Secondly, routines must be provided to find the expansion coefficients, or beam shape coefficients,  $a_{nm}$  and  $b_{nm}$  for the trapping beam. These are the following.

- (i) `bsc_pointmatch_farfield.m` and `bsc_pointmatch_focalplane.m`, described in (Nieminen *et al* 2003b), which can calculate the expansion coefficients for Gaussian beams, Laguerre–Gauss modes, and bi-Gaussian beams. Since these routines are much faster for rotationally symmetric beams, such as Laguerre–Gauss beams, a routine, `lgmodes.m`, that can provide the Laguerre–Gauss decomposition of an arbitrary paraxial beam is also provided.

- (ii) `bsc_plane.m`, for the expansion coefficients of a plane wave. This is not especially useful for optical trapping, but makes the toolbox more versatile, improving its usability for more general light scattering calculations.

Thirdly, the transformation matrices for the expansion coefficients under rotations and translations must be calculated. Routines include the following.

- (i) `wigner_rotation_matrix.m`, implementing the algorithm given by Choi *et al* (1999).
- (ii) `translate_z.m`, implementing the algorithm given by Videen (2000).

## 4. $T$ -matrix

For spherical particles, the usual Mie coefficients can be rapidly calculated. For non-spherical particles, a more intensive numerical effort is required. We use a least-squares overdetermined point-matching method (Nieminen *et al* 2003a). For axisymmetric particles, the method is relatively fast. However, as is common for many methods of calculating the  $T$ -matrix, particles cannot have extreme aspect ratios, and must be simple in shape. Typical particle shapes that we have used are spheroids and cylinders, and aspect ratios of up to four give good results. Although it can take a long time to calculate the  $T$ -matrix for general non-axisymmetric particles, it is possible to make use of symmetries such as mirror symmetry and discrete rotational symmetry to greatly speed up the calculation (Kahnert 2005, Nieminen *et al* 2006). We include a symmetry-optimized  $T$ -matrix routine for cubes.

Expanding the range of particles for which we can calculate the  $T$ -matrix is one of our current active research efforts, and we plan to include routines for anisotropic and inhomogeneous particles, and particles with highly complex geometries.

Once the  $T$ -matrix is calculated, the scattered field coefficients are simply found by a matrix–vector multiplication of the  $T$ -matrix and a vector of the incident field coefficients.

### 4.1. Implementation

Our  $T$ -matrix routines include the following.

- (i) `tmatrix_mie.m`, calculating the Mie coefficients for homogeneous isotropic spheres.
- (ii) `tmatrix_pm.m`, our general point-matching  $T$ -matrix routine.
- (iii) `tmatrix_pm_cube.m`, the symmetry-optimized cube code.

## 5. Optical force and torque

As noted earlier, the integrals of the momentum and angular momentum fluxes reduce to sums of products of the expansion coefficients. It is sufficient to give the formulae for the  $z$ -components of the fields, as given, for example, by Crichton and Marston (2000). We use the same formulae to calculate the  $x$  and  $y$  components of the optical force and torque, using 90° rotations of the coordinate system (Choi *et al* 1999). It is also possible to directly calculate the  $x$  and  $y$  components

using similar, but more complicated, formulae (Farsund and Felderhof 1996).

The axial trapping efficiency  $Q$  is

$$Q = \frac{2}{P} \sum_{n=1}^{\infty} \sum_{m=-n}^n \frac{m}{n(n+1)} \text{Re}(a_{nm}^* b_{nm} - p_{nm}^* q_{nm}) - \frac{1}{n+1} \left[ \frac{n(n+2)(n-m+1)(n+m+1)}{(2n+1)(2n+3)} \right]^{\frac{1}{2}} \times \text{Re}(a_{nm} a_{n+1,m}^* + b_{nm} b_{n+1,m}^* - p_{nm} p_{n+1,m}^* - q_{nm} q_{n+1,m}^*) \quad (10)$$

in units of  $n\hbar k$  per photon, where  $n$  is the refractive index of the medium in which the trapped particles are suspended. This can be converted to SI units by multiplying by  $nP/c$ , where  $P$  is the beam power and  $c$  is the speed of light in free space.

The *torque efficiency*, or normalized torque, about the  $z$ -axis acting on a scatterer is

$$\tau_z = \sum_{n=1}^{\infty} \sum_{m=-n}^n m(|a_{nm}|^2 + |b_{nm}|^2 - |p_{nm}|^2 - |q_{nm}|^2)/P \quad (11)$$

in units of  $\hbar$  per photon, where

$$P = \sum_{n=1}^{\infty} \sum_{m=-n}^n |a_{nm}|^2 + |b_{nm}|^2 \quad (12)$$

is proportional to the incident power (omitting a unit conversion factor which will depend on whether SI, Gaussian, or other units are used). This torque includes contributions from both spin and orbital components, which can both be calculated by similar formulae (Crichton and Marston 2000). Again, one can convert these values to SI units by multiplying by  $P/\omega$ , where  $\omega$  is the optical frequency.

### 5.1. Implementation

One routine, `forcetorque.m`, is provided for the calculation of the force, torque and spin transfer. The orbital angular momentum transfer is the difference between the torque and the spin transfer. The incoming and outgoing power (the difference being the absorbed power) can be readily calculated directly from the expansion coefficients, as can be seen from (12).

## 6. Miscellaneous routines

A number of other routines that do not fall into the above categories are included. These include the following.

- (i) Examples of use.
- (ii) Routines for conversion of coordinates and vectors from Cartesian to spherical and spherical to Cartesian.
- (iii) Routines to automate common tasks, such as finding the equilibrium position of a trapped particle, spring constants, and force maps.
- (iv) Functions required by other routines.

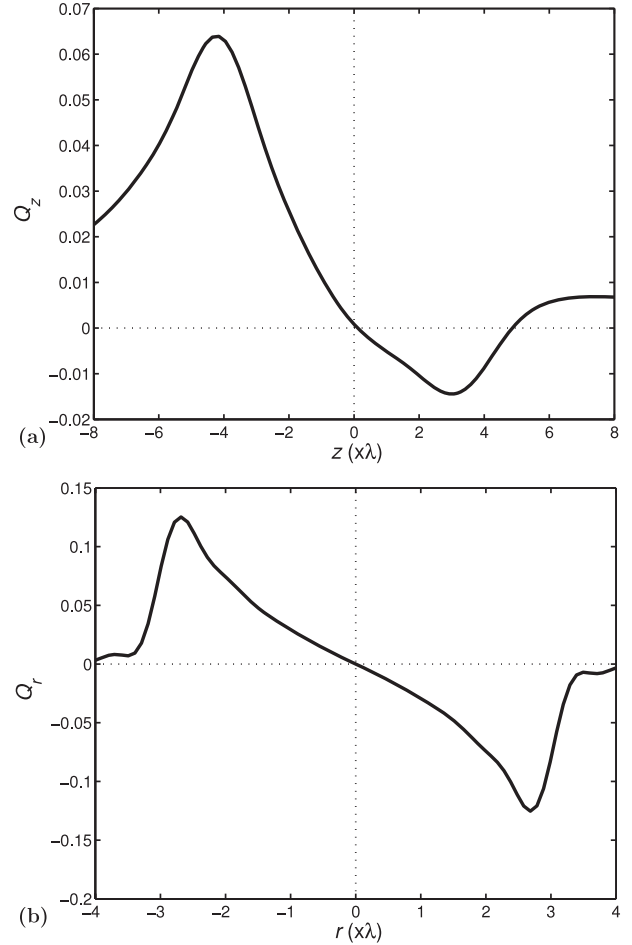


**Figure 1.** Gaussian trap (`example_gaussian.m`). Force on a sphere in a Gaussian beam trap. The half-angle of convergence of the  $1/e^2$  edge of the beam is  $50^\circ$ , corresponding to a numerical aperture of 1.02. The particle has a relative refractive index equal to  $n = 1.59$  in water, and has a radius of  $2.5 \lambda$ , corresponding to a diameter of  $4.0 \mu\text{m}$  if trapped at  $1064 \text{ nm}$  in water. (a) The axial trapping efficiency as a function of axial displacement and (b) the transverse trapping efficiency as a function of transverse displacement from the equilibrium point.

## 7. Typical use of the toolbox

Typically, for a given trap and particle, a  $T$ -matrix routine (usually `tmatrix_mie.m`) will be run once. Next, the expansion coefficients for the beam are found. Depending on the interests of the user, a function automating some common task, such as finding the equilibrium position within the trap, might be used, or the user might directly use the rotation and translation routines to enable calculation of the force or torque at desired positions within the trap.

The speed of calculation depends on the size of the beam, the size of the particle, and the distance of the particle from the focal point of the beam. Even for a wide beam and a large distance, the force and torque at a particular position can typically be calculated in much less than one second.

More complex tasks are possible, such as finding the optical force as a function of some property of the particle, which can, for example, be used to determine the refractive index of a microsphere (Knöner *et al* 2006).

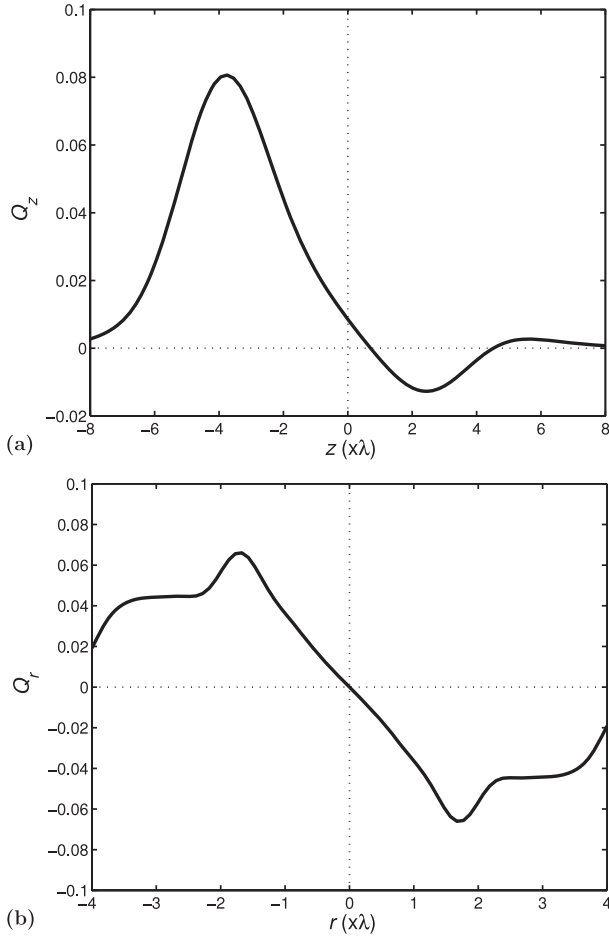


**Figure 2.** Laguerre–Gauss trap (`example_lg.m`). Force on a sphere in a Laguerre–Gauss beam trap. The half-angle of convergence of the  $1/e^2$  outer edge of the beam is  $50^\circ$ , as in figure 1. The sphere is identical to that in figure 1. (a) The axial trapping efficiency as a function of axial displacement and (b) the transverse trapping efficiency as a function of transverse displacement from the equilibrium point. Compared with the Gaussian beam trap, the radial force begins to drop off at smaller radial displacements, due to the far side of the ring-shaped beam no longer interacting with the particle.

Figures 1–4 demonstrate some of the capabilities of the toolbox. Figure 1 shows a simple application—the determination of the force as a function of axial displacement from the equilibrium position in a Gaussian beam trap. Figure 2 shows a similar result, but for a particle trapped in a Laguerre–Gauss  $LG_{03}$  beam. Figure 3 shows a more complex application, with repeated calculations (each similar to the one shown in figure 1(a)) being used to determine the effect of the combination of relative refractive index and particle size on trapping. Finally, figure 4 shows the trapping of a non-spherical particle, a cube.

Agreement with precision experimental measurements suggests that errors of less than 1% are expected.

## 8. Future development

We are actively engaged in work to extend the range of particles for which we can model trapping. This currently includes birefringent particles and particles of arbitrary

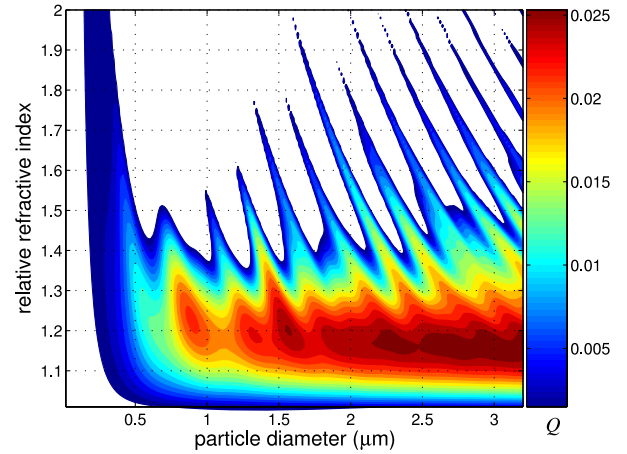


**Figure 3.** Trapping landscape (`example_landscape.m`). The maximum axial restoring force for displacement in the direction of beam propagation is shown, in terms of the trapping efficiency as a function of relative refractive index and microsphere diameter. The trapping beam is at 1064 nm and is focused by an  $NA = 1.2$  objective. This type of calculation is quite slow, as the trapping force as a function of axial displacement must be found for a grid of combinations of relative refractive index and sphere diameter. On the left-hand side, we can see that the trapping force rapidly becomes very small as the particle size becomes small—the gradient force is proportional to the volume of the particle for small particles. In the upper portion, we can see that whether or not the particle can be trapped strongly depends on the size—for particular sizes, reflection is minimized, and even high index particles can be trapped.

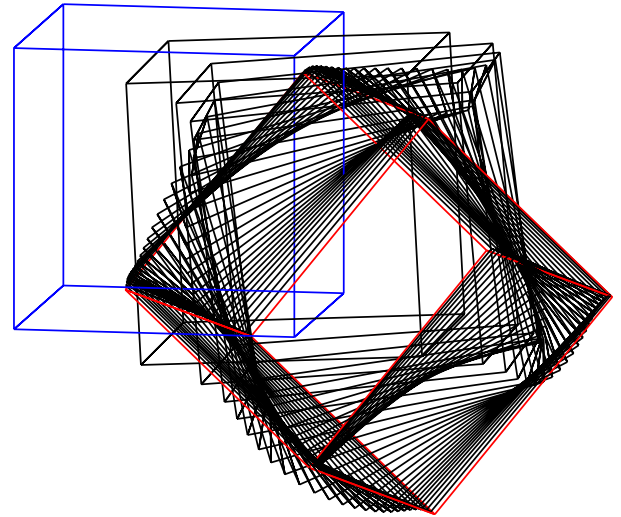


**Figure 4.** Optical trapping of a cube (`example_cube.m`). A sequence showing the optical trapping of a cube. The cube has faces of  $2\lambda/n_{\text{medium}}$  across, and has a refractive index of  $n = 1.59$ , and is trapped in water. Since the force and torque depend on the orientation as well as position, a simple way to find the equilibrium position and orientation is to ‘release’ the cube and calculate the change in position and orientation for appropriate time steps. The cube can be assumed to always be moving at terminal velocity and terminal angular velocity (Nieminen *et al* 2001a). The cube begins face up, centred on the focal plane of the beam, and to one side. The cube is pulled into the trap and assumes a corner-up orientation. The symmetry optimizations allow the calculation of the  $T$ -matrix in 20 min; otherwise, 30 h would be required. Once the  $T$ -matrix is found, successive calculations of the force and torque require far less time, on the order of a second or so.



geometry. Routines to calculate the  $T$ -matrices for such particles will be included in the main code when available.

Other areas in which we aim to further improve the toolbox are robust handling of incorrect or suspect input, more automation of tasks, and GUI tools.

We also expect feedback from the optical trapping and micromanipulation community to help us add useful routines and features.

## References

- Abraham M 1909 *Rend. Circolo Mat. Palermo* **28** 1–28
- Abraham M 1910 *Rend. Circolo Mat. Palermo* **30** 33–46
- Ashkin A 1992 *Biophys. J.* **61** 569–82
- Barnett S M 2002 *J. Opt. B: Quantum Semiclass. Opt.* **4** S7–16
- Barnett S M and Loudon R 2006 *J. Phys. B: At. Mol. Opt. Phys.* **39** S671–84
- Bayouth S, Nieminen T A, Heckenberg N R and Rubinshtein-Dunlop H 2003 *J. Mod. Opt.* **50** 1581–90
- Bishop A I, Nieminen T A, Heckenberg N R and Rubinshtein-Dunlop H 2003 *Phys. Rev. A* **68** 033802
- Bishop A I, Nieminen T A, Heckenberg N R and Rubinshtein-Dunlop H 2004 *Phys. Rev. Lett.* **92** 198104
- Bohren C F 1995 *Handbook of Optics* 2nd edn, vol 1, ed M Bass, E W Van Stryland, D R Williams and W L Wolfe (New York: McGraw-Hill) chapter 6, pp 6.1–21
- Brevik I 1979 *Phys. Rep.* **52** 133–201
- Brock B C 2001 Using vector spherical harmonics to compute antenna mutual impedance from measured or computed fields *Sandia Report SAND2000-2217-Revised* Sandia National Laboratories, Albuquerque, NM
- Chaumet P C, Rahmani A, Sentenac A and Bryant G W 2005 *Phys. Rev. E* **72** 046708
- Choi C H, Ivanic J, Gordon M S and Ruedenberg K 1999 *J. Chem. Phys.* **111** 8825–31
- Collett W L, Ventrice C A and Mahajan S M 2003 *Appl. Phys. Lett.* **82** 2730–2
- Crichton J H and Marston P L 2000 *Electron. J. Diff. Eqns Conf.* **04** 37–50
- de Groot S R and Suttorp L G 1972 *Foundations of Electrodynamics* (Amsterdam: North-Holland)
- Doicu A and Wriedt T 1997 *Appl. Opt.* **36** 2971–8
- Farsund Ø and Felderhof B U 1996 *Physica A* **227** 108–30
- Gauthier R C 2005 *Opt. Express* **13** 3707–18
- Gordon J P 1973 *Phys. Rev. A* **8** 14–21
- Gouesbet G and Gréhan G 1982 *J. Opt. (Paris)* **13** 97–103
- Grzegorzczak T M, Kemp B A and Kong J A 2006 *J. Opt. Soc. Am. A* **23** 2324–30
- Gumerov N A and Duraiswami R 2003 *SIAM J. Scientific Comput.* **25** 1344–81
- Han Y, Gréhan G and Gouesbet G 2003 *Appl. Opt.* **42** 6621–9
- Han Y and Wu Z 2001 *Appl. Opt.* **40** 2501–9
- Harada Y and Asakura T 1996 *Opt. Commun.* **124** 529–41
- Hoekstra A G, Frijlink M, Waters L B F M and Sloot P M A 2001 *J. Opt. Soc. Am. A* **18** 1944–53
- Humblert J 1943 *Physica* **10** 585–603
- Jackson J D 1999 *Classical Electrodynamics* 3rd edn (New York: Wiley)
- Jauch J M and Rohrlich F 1976 *The Theory of Photons and Electrons* 2nd edn (New York: Springer)
- Jones R V 1978 *Proc. R. Soc. Lond. A* **360** 365–71
- Kahnert F M 2003 *J. Quant. Spectrosc. Radiat. Transfer* **79/80** 775–824
- Kahnert M 2005 *J. Opt. Soc. Am. A* **22** 1187–99
- Knöner G, Parkin S, Nieminen T A, Heckenberg N R and Rubinshtein-Dunlop H 2006 *Phys. Rev. Lett.* **97** 157402
- Leonhardt U 2006 *Nature* **444** 823–4
- Lock J A 2004a *Appl. Opt.* **43** 2532–44
- Lock J A 2004b *Appl. Opt.* **43** 2545–54
- Lorenz L 1890 *Vidensk. Selsk. Skr.* **6** 2–62
- Loudon R and Barnett S M 2006 *Opt. Express* **14** 11855–69
- Maia Neto P A and Nussenzweig H M 2000 *Europhys. Lett.* **50** 702–8
- Mansuripur M 2004 *Opt. Express* **12** 5375–401
- Mansuripur M 2005 *Opt. Express* **13** 5315–24
- Mansuripur M 2007 *Opt. Express* **15** 2677–82
- Mazolli A, Maia Neto P A and Nussenzweig H M 2003 *Proc. R. Soc. Lond. A* **459** 3021–41
- Mie G 1908 *Ann. Phys., Lpz.* **25** 377–445
- Minkowski H 1908 *Nachr. Gess. Wiss. Gött. Math. Phys. Klasse* **1908** 53–111
- Mishchenko M I 1991 *J. Opt. Soc. Am. A* **8** 871–82
- Mishchenko M I, Travis L D and Lacis A A 2002 *Scattering, Absorption, and Emission of Light by Small Particles* (Cambridge: Cambridge University Press)
- Mishchenko M I, Videen G, Babenko V A, Khlebtsov N G and Wriedt T 2004 *J. Quant. Spectrosc. Radiat. Transfer* **88** 357–406
- Moine O and Stout B 2005 *J. Opt. Soc. Am. B* **22** 1620–31
- Neves A A R, Fontes A, Pozzo L d, de Thomaz A A, Chille E, Rodriguez E, Barbosa L C and Cesar C L 2006 *Opt. Express* **14** 13101–6
- Nieminen T A, Heckenberg N R and Rubinshtein-Dunlop H 2001a *J. Mod. Opt.* **48** 405–13
- Nieminen T A, Heckenberg N R and Rubinshtein-Dunlop H 2004 *Proc. SPIE* **5514** 514–23
- Nieminen T A, Loke V L Y, Brańczyk A M, Heckenberg N R and Rubinshtein-Dunlop H 2006 *PIERS Online* **2** 442–6
- Nieminen T A, Rubinshtein-Dunlop H and Heckenberg N R 2001b *J. Quant. Spectrosc. Radiat. Transfer* **70** 627–37
- Nieminen T A, Rubinshtein-Dunlop H and Heckenberg N R 2003a *J. Quant. Spectrosc. Radiat. Transfer* **79/80** 1019–29
- Nieminen T A, Rubinshtein-Dunlop H and Heckenberg N R 2003b *J. Quant. Spectrosc. Radiat. Transfer* **79/80** 1005–17
- Nieminen T A, Rubinshtein-Dunlop H, Heckenberg N R and Bishop A I 2001a *Comput. Phys. Commun.* **142** 468–71
- Padgett M, Barnett S M and Loudon R 2003 *J. Mod. Opt.* **50** 1555–62
- Penfield P Jr and Haus H A 1967 *Electrodynamics of Moving Media* (Cambridge, MA: MIT)
- Pfeifer R N C, Nieminen T A, Heckenberg N R and Rubinshtein-Dunlop H 2006 *Proc. SPIE* **6326** 63260H
- Ren K F, Gréhan G and Gouesbet G 1996 *Appl. Opt.* **35** 2702–10
- Simpson S H and Hanna S 2006 *J. Opt. Soc. Am. A* **23** 1419–31
- Simpson S H and Hanna S 2007 *J. Opt. Soc. Am. A* **24** 430–43
- Singer W, Nieminen T A, Gibson U J, Heckenberg N R and Rubinshtein-Dunlop H 2006 *Phys. Rev. E* **73** 021911
- Soper D E 1976 *Classical Field Theory* (New York: Wiley)
- Stewart A M 2005 *Eur. J. Phys.* **26** 635–41
- Sun W, Pan S and Jiang Y 2006 *J. Mod. Opt.* **53** 2691–700
- Tsang L 2001 *Scattering of Electromagnetic Waves* 3 volumes (New York: Wiley)
- Umov N A 1950 *Izbrannye Sochineniya (Selected Works)* (Moscow: Gostexizdat) (in Russian)
- van de Hulst H C 1957 *Light scattering by small particles* (New York: Wiley)
- Videen G 2000 Light Scattering from Microstructures number 534 *Lecture Notes in Physics* ed F Moreno and F González (Berlin: Springer) chapter 5, pp 81–96
- Waterman P C 1971 *Phys. Rev. D* **3** 825–39
- White D A 2000a *J. Comput. Phys.* **159** 13–37
- White D A 2000b *Comput. Phys. Commun.* **128** 558–64
- Wohland T, Rosin A and Stelzer E H K 1996 *Optik* **102** 181–90
- Wong V and Ratner M A 2006 *J. Opt. Soc. Am. B* **23** 1801–14
- Wriedt T 1998 *Part. Part. Syst. Charact.* **15** 67–74
- Zambrini R and Barnett S M 2005 *J. Mod. Opt.* **52** 1045–52